International Journal of Technology 10(8): 1593-1601
ISSN 2086-9614

EFFECT OF FEED METAL FLOW RATE ON LOW-COST PLASMA ATOMIZER FOR FABRICATING 316L STAINLESS STEEL POWDER

Dharmanto,[1] Sugeng Supriadi,[1] Ario Sunar Baskoro[1*]

[1]*Department of Mechanical Engineering, Faculty of Engineering, Universitas Indonesia, Kampus UI Depok, Depok 16424, Indonesia*

(Received: March 2019 / Revised: September 2019 / Accepted: November 2019)

ABSTRACT

The low-cost plasma atomizer in the present study successfully synthesized stainless steel spherical powder using an energy source of less than 3 kVA. Repeated testing was conducted to examine the resulting spherical powder, among other observations, using a digital microscope (Dino-Lite AM4115), scanning electron microscopy (SEM-FEI-Inspect F50), and energy dispersive spectroscopy (EDS). To ensure the purity of the resulting 316L stainless steel spherical powder, EDS was used for qualitative and quantitative elemental analysis. The results showed that the 316L stainless steel spherical powder particles varied in size from 26 µm to 180 µm with average particle diameters of approximately 82.6 µm, making them ideal for biomedical applications. The results of the feed metal flow rate on the powder weight percentages for particle sizes <50 µm for 2 mm^3/s feed metal flow, 3 mm^3/s feed metal flow, and 4 mm^3/s feed metal flow were 26.04%, 28.04%, and 13.09%, respectively. It is possible that this could occur because greater metal flow rates require greater plasma energy to form liquid metal droplets, so that a lower metal flow rate at the same energy consumption makes it possible to produce more metal powder in smaller particles.

Keywords: Plasma atomizer; Powder technology; Spherical particle; Stainless steel powder

1. INTRODUCTION

The metal manufacturing industry is currently interested in developing metal powder technology for production cost efficiency. One of the applications of metal powder technology is as a feedstock for metal injection molding (MIM) (Suharno et al., 2019; Supriadi et al., 2019). MIM can produce lower surface roughness values compared to investment casting (Suharno et al., 2018). MIM is advantageous mainly due to its significant technological cost savings compared with the use of machinery (Schieleper, 2006; Supriadi et al., 2015). Metal powder technology enables reductions in waste material production. Metal powder technology can be classified as a green technology because it can reduce more residual waste material than other conventional fabrication technologies such as five-axis CNC machining (Higashitani et al., 2019). At this time, the atomization process is a suitable choice for producing metal powder because atomization is capable of producing large amounts of powder with high purity (Boulos, 2004). Atomization processes for making metal powder include water atomization, gas atomization (Zhao et al., 2007), centrifugal atomization (Sungkhaphaitoon et al., 2013), plasma atomization, and plasma rotating electrodes process atomization (Dawes et al., 2015).

The atomization process that uses a plasma arc has a high heat source density that can melt various

*Corresponding author's email: ario@eng.ui.ac.id, Tel. +62-21-7270032, Fax. +62-21-7270033
Permalink/DOI: https://dx.doi.org/10.14716/ijtech.v10i8.3476

metals with a high melting point (Lü et al., 2013). The plasma arc used in this study was a type of thermal plasma that is commonly used, including in cutting (Wang et al., 2000), welding (Luo, 2003), surface hardening (Ismail & Taha, 2014), nanopowder synthesis (Liu et al., 2015; Saryanto & Sebayang, 2017), and surface treatment of biomedical materials (Chu et al., 2002).

A plasma atomizer is capable of producing a powder with particle diameters of 50 µm (Chen et al., 2018). Powder with particles of this size can be applied as the primary raw material for making medical devices (Grenier & Allaire, 1997; Baskoro & Supriadi, 2019). One of the characteristics of high-quality metal powder is the perfect spherical shapes of the particles and a narrow size distribution, which can improve the flowability of the powder.

The current challenge of using plasma atomization is its high cost, partly because the process requires a large energy source. The energy sources used generally have a power of approximately 20 kVA-600 kVA (Tsantrizos et al., 1998; Dignard & Boulos, 2000; Boulos, 2004; Dawes et al., 2015). In the present study, a plasma atomizer with low-cost equipment was designed and built as a solution to the high cost of plasma atomization. A plasma atomizer was fabricated with a power of 3 kVA without the need to use a melt bath, so the plasma atomization process is faster than the gas atomization or water atomization processes. The plasma atomization process has been made to produce stainless steel spherical powder particles with a diameter of less than 50 µm.

2. METHODS

The raw material used in the plasma atomization process is 316L stainless steel wire, which is a type of medical grade (Chen et al., 2018). The plasma atomizer successfully produced 316L stainless steel spherical powder. Figure 1 shows that the plasma atomizer was operated with less than a 3 kVA plasma power source. The plasma atomizer consists of six main elements: direct current (DC) plasma, a feeder motor, a plasma nozzle, a chamber, a suction blower, and cyclones.

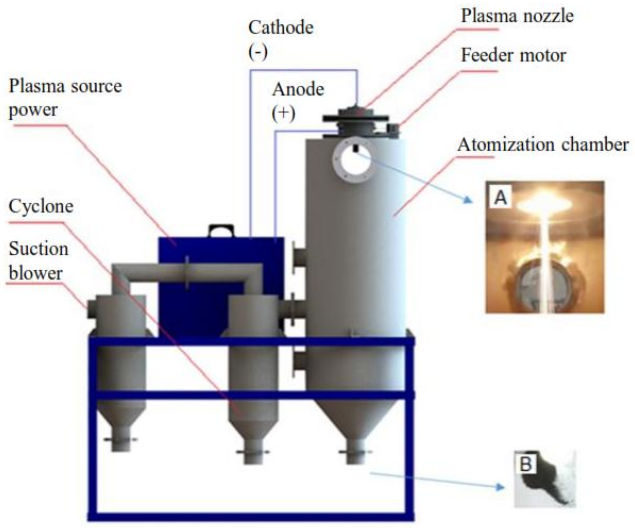

Figure 1 The design of the low-cost plasma atomizer: (a) Atomization plasma arc; (b) 316L stainless steel spherical powder results

A feeder motor fed metal wire into the plasma nozzle at 2 mm^3/s feed metal flow, 3 mm^3/s feed metal flow, and 4 mm^3/s feed metal flow. The feed metal material was in the form of wire of approximately 1.6 mm diameter that was continuously driven forward by a DC motor. The tip of the wire, which was in the plasma conduit, was heated and melted in the presence of a plasma arc. The melted metal was carried away by the plasma arc jet gas out of the plasma conduit so that the droplets were formed, and the melted metal droplets were scattered in the chamber

reactor, forming spherical particles of stainless steel. The electrical current source for the plasma was 25 ampere. The DC current measurement instrument was an Amprobe LH41A DC low-current, clamp-on ammeter with a basic accuracy of ±1.3% + 3 digits.

Repeated testing was conducted to examine the resulting spherical powder, among other observations, using a digital microscope (Dino-Lite AM4115), scanning electron microscopy (SEM-FEI-Inspect F50), and energy dispersive spectroscopy (EDS). To ensure the purity of the 316L stainless steel spherical powder results, EDS was used for qualitative and quantitative elemental analysis.

3. RESULTS AND DISCUSSION

The resulting 316L stainless steel spherical powder particles varied from 26 µm to 180 µm, which can be seen in the digital microscope images in Figure 2. Figure 3 shows the morphology and size of the 316L stainless steel spherical powder particles. The average particle diameter was approximately 82.6 µm, making the powder ideal for biomedical applications (Grenier & Allaire, 1997).

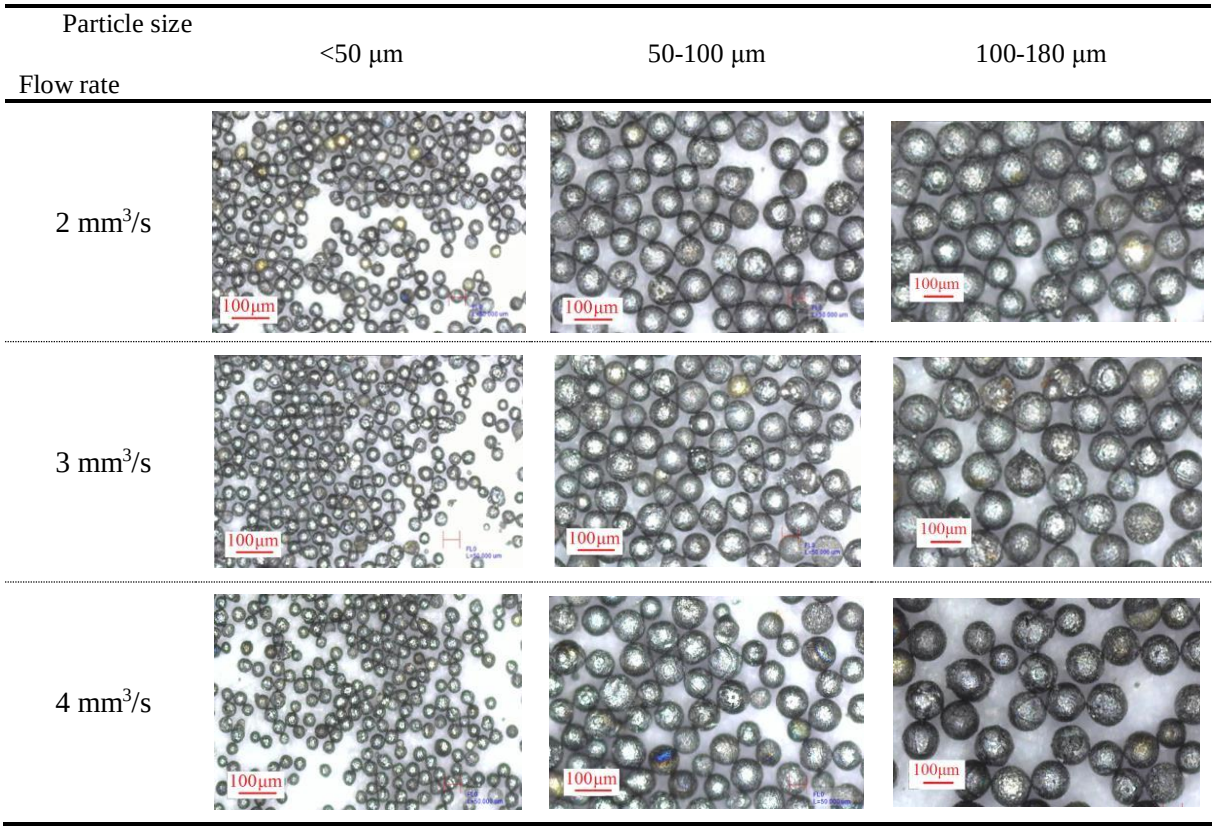

Figure 2 Digital microscope images of 316L stainless steel spherical powder

Based on the SEM results, there is a porosity measuring approximately 1–7 µm. This may be because if there is any turbulence in the metal movement that allows air bubbles to be trapped in the metal, these bubbles will remain trapped when the metal solidifies (Tammas-Williams et al., 2016; Brooks et al., 2017; Cunningham et al., 2017a; Cunningham et al., 2017b).

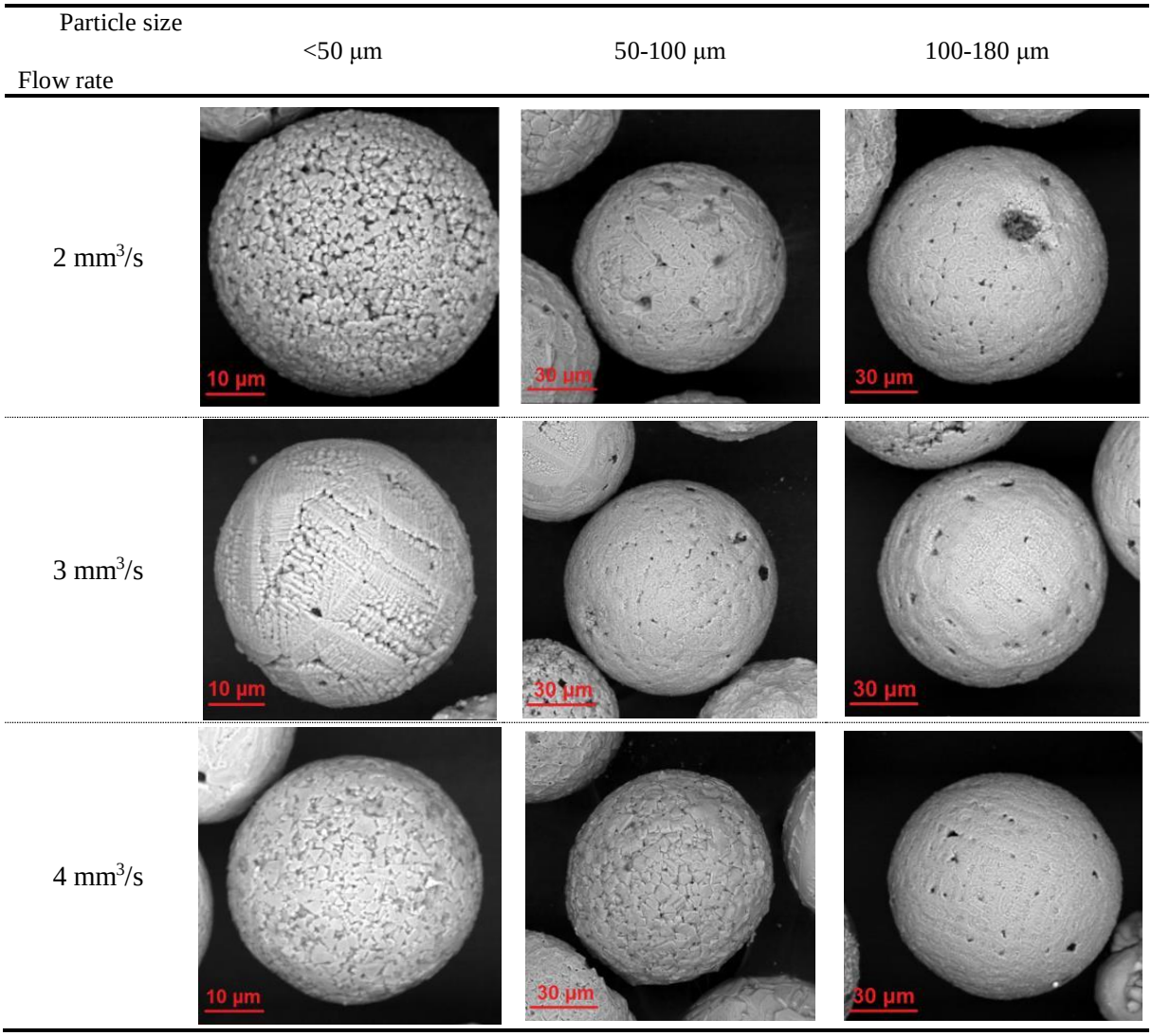

Figure 3 SEM results of 316L stainless steel spherical powder

The values shown in the graph in Figure 4 are the conversion results from the gram to the weight percentage (wt %) for each filtered powder particle, the mesh sizes of which are #100, #200, and #325, which have also been converted into micrometers, namely 100–180 µm, 50–100 µm, and <50 µm, respectively.

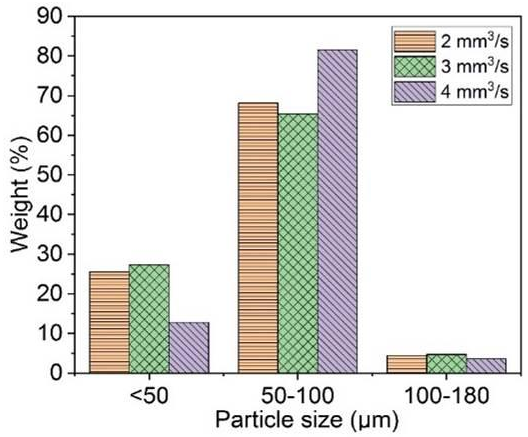

Figure 4 Effect of metal flow rate on the 316L stainless steel powder particle size distribution

Figure 4 shows the comparison graph of the particle size distribution for each of the melt flow rates, which shows that the 50-100 μm powder has the highest weight percentage, followed by the <50 μm powder. The particle size of the metal powder commonly used in the metal injection molding process is ≤45μm (Heaney, 2012). The results of the feed metal flow rate on the powder weight percentages for particle sizes <50 μm for 2 mm^3/s feed metal flow, 3 mm^3/s feed metal flow, and 4 mm^3/s feed metal flow were 26.04%, 28.04%, and 13.09%, respectively. It is possible that this could occur because greater metal flow rates require greater plasma energy to form liquid metal droplets and, at lower metal flow rates, it is possible to produce more metal powder of smaller particles.

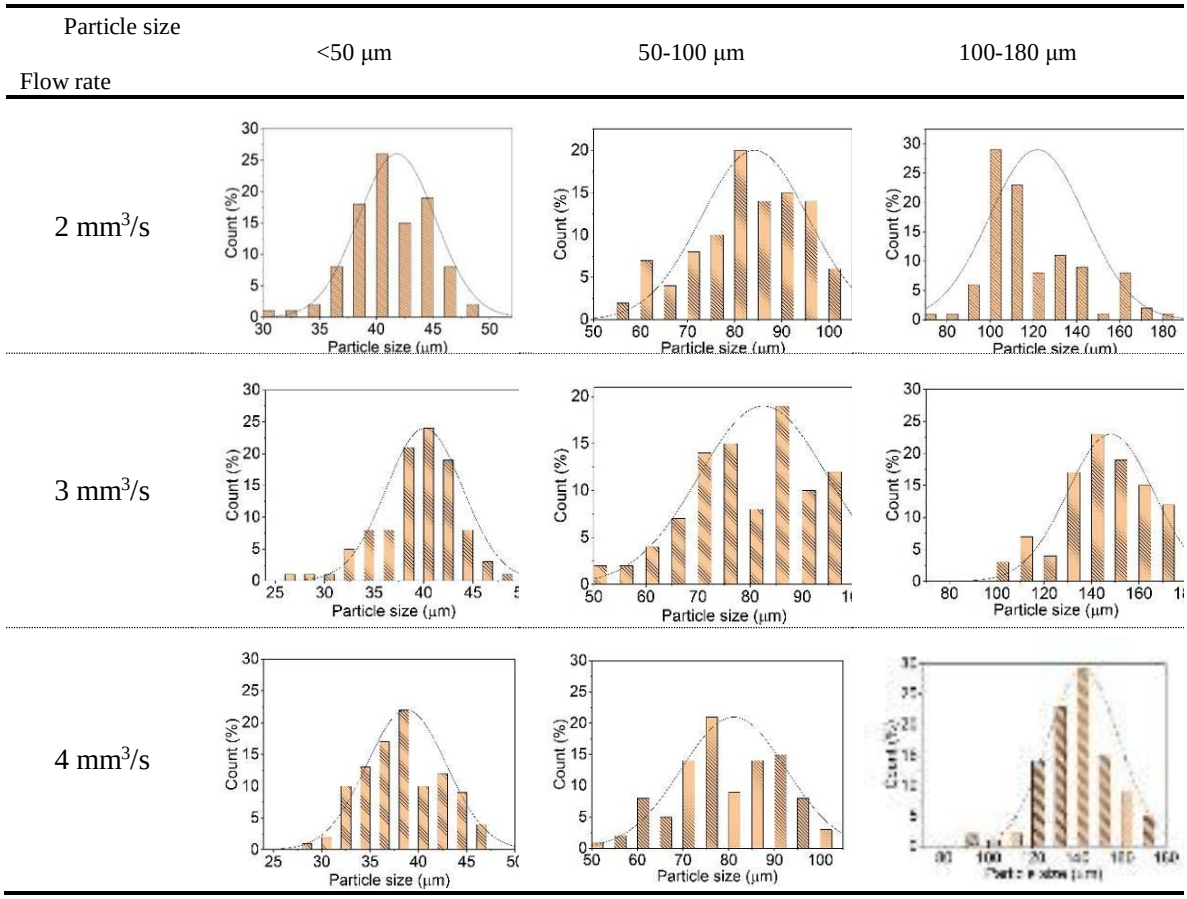

Figure 5 The particle size distribution of the 316L stainless steel powder

Figure 5 shows the particle size distribution of the powder at metal feed rates of 2 mm^3/s, 3 mm^3/s, and 4 mm^3/s. The particle size distribution of <50 μm has the highest count, almost the same for all variations, at approximately 38-40 μm, whereas the particle size distribution of 50-100 μm has the highest count, almost the same for all variations, at approximately 78–90 μm. However, the particle size distribution of 100–180 μm at 2 mm^3/s feed metal flow, 3 mm^3/s feed metal flow, and 4 mm^3/s feed metal flow had the highest counts of100 μm, 140 μm, and 140 μm, respectively.

Figure 6 shows a comparison of the stainless steel powder produced using the low-cost plasma atomization method developed in this study with commercial stainless steel powder from Epson Atmix Corp. in Japan. While the low-cost plasma atomizer can produce more perfectly spherical stainless steel particles, there are no satellites attached to the particles but more pores than in commercial stainless steel powder particles. On the other hand, porous stainless steel particles can be advantageous in making metal implants in orthopedic surgery. So it was deliberately done to overcome the problem of incompatibility between the modulus of elasticity of 316L stainless steel implants (210 GPa) and the modulus of elasticity of natural bone (10–30 GPa) (Becker &

D Bolton, 1997; Hutmacher, 2000). The modulus of elasticity and strength of 316L stainless steel can be controlled using porous materials with various porosities to match the modulus of elasticity and strength of natural bone (Dewidar, 2012).

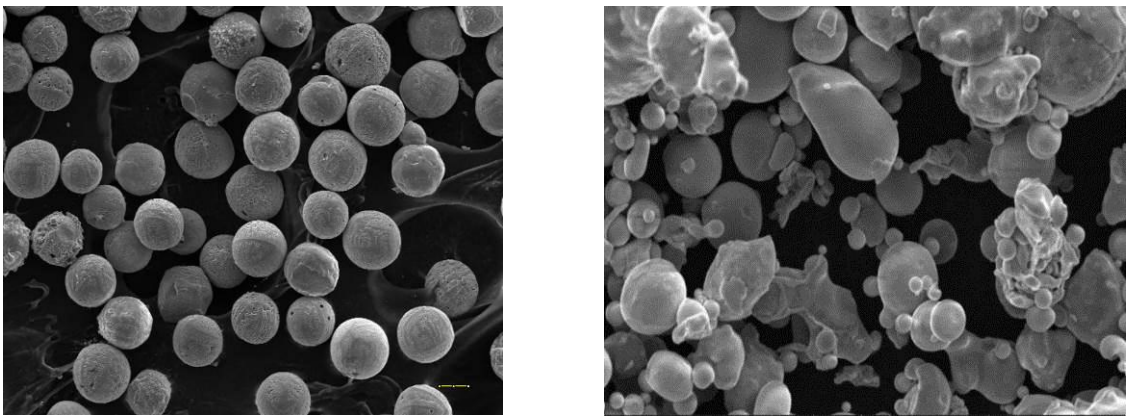

(a) (b)

Figure 6 (a) SEM of stainless steel powder result of low-cost plasma atomization; (b) SEM of commercial stainless steel powder

Figure 7 shows the EDS results of the 316L stainless steel powder, which had chrome and nickel contents of 17.9 wt% and 13.1 wt%, respectively, while the initial composition of the 316L stainless steel powder had chrome and nickel contents of 18.15 wt% and 11.17 wt%, respectively.

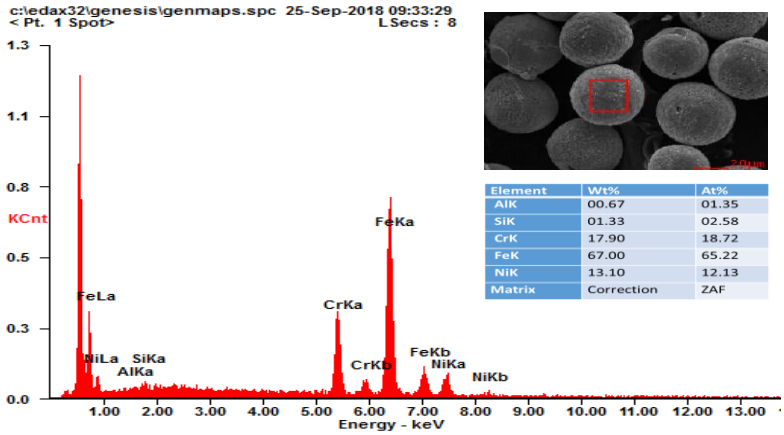

Figure 7 EDS results of 316L stainless steel spherical powder on powder surfaces

The ratio of plasma energy used in the plasma atomization process on the 316L stainless steel material had weight ranges of 20.7 g/kWh to 41.5 g/kWh. On the other hand, some studies of energy consumption from existing plasma atomization have showed a value of the energy-to-weight ratio of between 19 g/kWh and 32 g/kWh (Tsantrizos et al., 1998) and 34.96 g/kWh (Dion & Francois, 2019). The plasma atomizer is operated with plasma resources of less than 3 kVA, so the plasma atomization in this study can be called low-cost plasma atomization.

In addition, based on visual observations of plasma arcs during the atomization process, sometimes instability of plasma arcs is seen. Plasma arc instability is possible due to erosion that occurs at the cathode or the anode, so the distance between the cathode and the anode becomes far (Knight et al., 1991). An automatic device for adjusting the gap between the cathode and the anode, it is possible to create a machine vision system based on the characteristic brightness range to detect the edge of the plasma arc by using the camera as a plasma arc flame sensor (Baskoro et al., 2011; Baskoro et al., 2016; Baskoro & Supriadi, 2019).

4. CONCLUSION

The results of the experiments in this study show that the plasma atomizer successfully synthesized the spherical metal powder using an energy source of less than 3 kVA. The plasma atomizer can produce perfectly spherical stainless steel powder particles. The sizes of the resulting 316L stainless steel spherical powder particles vary from 26 µm to 180 µm. The average particle diameter is approximately 82.6 µm. The results of the flow rate on the powder weight percentages at particle sizes <50 µm for 2 mm^3/s feed metal flow, 3 mm^3/s feed metal flow, and 4 mm^3/s feed metal flow are 26.04%, 28.04%, and 13.09%, respectively. It is possible that this could occur because greater metal flow rates require greater plasma energy to form liquid metal droplets, so that a lower metal flow rate makes it possible to produce more metal powder in smaller particles. The resulting 316L stainless steel spherical powder is likely to be used in biomedical manufacturing applications. Based on the above research, fascinating research could be conducted to find the optimal parameters in the plasma atomization in order to produce particle sizes that are suitable for biomedical equipment manufacturing applications.

5. ACKNOWLEDGEMENT

This research was supported by the Ministry of Research and Technology of the Republic of Indonesia through the Excellent Applied Research in Higher Education scheme (contract number: NKB-1744/ UN2.R3.1/ HKP.05.00/ 2019).

6. REFERENCES

Baskoro, A.S., Masuda R., Suga Y., 2011. Comparison of Particle Swarm Optimization and Genetic Algorithm for Molten Pool Detection in Fixed Aluminum Pipe Welding. *International Journal of Technology*, Volume 2(1), pp. 74–83

Baskoro, A.S., Supriadi S., 2019. Review on Plasma Atomizer Technology for Metal Powder. *In:* Proceedings of the MATEC Web of Conferences, 2019: EDP Sciences, 05004

Baskoro A.S., Tandian R., Edyanto A., Saragih A.S., 2019. Automatic Tungsten Inert Gas (TIG) Welding using Machine Vision and Neural Network on Material SS304. *In*: Proceedings of the 2016 International Conference on Advanced Computer Science and Information Systems (ICACSIS), 2016: IEEE, pp. 427–32

Becker, B., D Bolton J., 1997. Corrosion Behaviour and Mechanical Properties of Functionally Gradient Materials Developed for Possible Hard-tissue Applications. *Journal of Materials Science: Materials in Medicine*, Volume 8(12), pp. 793–797

Boulos, M., 2004. *Plasma Power Can Make Better Powders*. Metal Powder Report 59, pp. 16–21

Brooks, A. J., Ge J., Kirka M. M., Dehoff R. R., Bilheux H. Z., Kardjilov N., Manke I., Butler, L.G., 2017. Porosity Detection in Electron Beam-melted Ti-6Al-4V using High-resolution Neutron Imaging and Grating-based Interferometry. *Progress in Additive Manufacturing*, Volume 2(3), pp. 125–132

Chen, G., Zhao, S., Tan, P., Wang, J., Xiang, C., Tang, H., 2018. A Comparative Study of Ti-6Al-4V Powders for Additive Manufacturing by Gas Atomization, Plasma Rotating Electrode Process and Plasma Atomization. *Powder Technology*, Volume 333, pp. 38–46

Chu, P.K., Chen, J., Wang, L., Huang, N., 2002. *Plasma-surface Modification of Biomaterials*. Materials Science and Engineering: R: Reports 36, pp. 143–206

Cunningham, R., Narra, S.P., Montgomery, C., Beuth, J., Rollett, A., 2017a. Synchrotron-based X-ray Microtomography Characterization of the Effect of Processing Variables on Porosity Formation in Laser Power-bed Additive Manufacturing of Ti-6Al-$_4$V. *JOM*, Volume 69(3), pp. 479–484

Cunningham, R., Nicolas, A., Madsen, J., Fodran, E., Anagnostou, E., Sangid, M.D., Rollett, A.D., 2017b. Analyzing the Effects of Powder and Post-processing on Porosity and Properties of Electron Beam Melted Ti-6Al-$_4$V. *Materials Research Letters*, Volume 5(7), pp. 516–525

Dawes, J., Bowerman, R., Trepleton, R., 2015. Introduction to the Additive Manufacturing Powder Metallurgy Supply Chain. *Johnson Matthey Technology Review*, Volume 59(3), pp. 243–256

Dewidar, M., 2012. Influence of Processing Parameters and Sintering Atmosphere on the Mechanical Properties and Microstructure of Porous 316L Stainless Steel for Possible Hard-tissue Applications. *International Journal of Mechanical & Mechatronics Engineering*, Volume 12, pp. 10–24

Dignard, N., Boulos, M., 2000. Powder Spheroidization using Induction Plasma Technology. *In:* Proceedings of the ITSC 2000: 1st International Thermal Spray Conference, 2000, pp. 887–893

Dion, D.A.C., Francois, P., 2019. *Method for Cost-Effective Production of Ultrafine Spherical Powders at Large Scale using Thruster-assisted Plasma Atomization.* Google Patents

Grenier, S., Allaire, F., 1997. *Plasma Atomization Gives Unique Spherical Powders*. Metal Powder Report 52, pp. 34–37

Heaney, D., 2012. *Designing for Metal Injection Molding (MIM)*. Handbook of Metal Injection Molding. Elsevier, pp. 29–49

Higashitani, K., Makino, H., Matsusaka, S., 2019. *Powder Technology Handbook*. CRC Press.

Hutmacher, D.W., 2000. *Scaffolds in Tissue Engineering Bone And Cartilage*. The Biomaterials: Silver Jubilee Compendium. Elsevier, 175–189

Ismail, M.I.S., Taha, Z., 2014. Surface Hardening of Tool Steel by Plasma Arc with Multiple Passes. *International Journal of Technology*, Volume 5(1), pp. 79–87

Knight, R., Smith, R., Apelian, D., 1991. Application of Plasma Arc Melting Technology to Processing of Reactive Metals. *International Materials Reviews*, Volume 36(1), pp. 221–252

Liu, S.X., Liu, J.L., Li, X.S., Zhu, X., Zhu, A.M., 2015. Gliding Arc Plasma Synthesis of Visible–Light Active C-doped Titania Photocatalysts. *Plasma Processes and Polymers*, Volume 12(5), pp. 422–430

Lü, Y.-H., Liu, Y.-X., Xu, F.-J., Xu, B.-S., 2013. Plasma Transferred Arc Forming Technology for Remanufacture. *Advances in Manufacturing*, Volume 1(2), pp. 187–190

Luo, W., 2003. The Corrosion Resistance of 0Cr19Ni9 Stainless Steel Arc Welding Joints with and Without Arc Surface Melting. *Materials Science and Engineering: A*, Volume 345(1–2), pp. 1–7

Saryanto, H., Sebayang, D., 2017. The Simple Fabrication of Nanorods Mass Production for the Dye-sensitized Solar Cell. *In:* Proceedings of the MATEC Web of Conferences, 2017: EDP Sciences, 03006

Schieleper, G., 2006. *A Manufacturing Process for Precision Engineering Components.* Powder Metallurgy Association, United Kingdom

Suharno, B., Mawardi, F., Dewantoro, S., Irawan, B., Doloksaribu, M., Supriadi, S., 2019. Effect of Powder Loading on Local Feedstock Injection Behavior for Fabrication Process of Orthodontic Bracket SS 17-4 PH using Metal Injection Molding. *In:* Proceedings of the AIP Conference Proceedings, 2019: AIP Publishing, 020030

Suharno, B., Suharno, L.P., Saputro, H.R., Irawan, B., Prasetyadi, T., Ferdian, D., Supriyadi, S., 2018. Surface Quality and Microstructure of Low-vacuum Sintered Orthodontic Bracket 17-4 PH Stainless Steel Fabricated by MIM Process. *In:* Proceedings of the AIP Conference Proceedings, 2018: AIP Publishing, 020009

Sungkhaphaitoon, P., Likhidkan W., Kitjaidiaw S., Wisutmethangoon S., Plookphol T., 2013. Effect of Atomizer Disc Geometry on Zinc Metal Powder Production by Centrifugal

Atomization. *In:* Proceedings of the Applied Mechanics and Materials, Volume 271–272, pp. 232–236

Supriadi, S., Dewantoro, S., Mawardi, F. A., Irawan, B., Doloksaribu, M., Suharno, B., 2019. Preparation of Feedstock using Beeswax Binder and SS 17-4PH Powder for Fabrication Process of Orthodontic Bracket by Metal Injection Molding. *In:* Proceedings of the AIP Conference Proceedings, 2019: AIP Publishing, 020029

Supriadi S., Sitanggang T.W., Irawan B., Suharno B., Kiswanto G., Prasetyadi T., 2015. Orthodontic Bracket Fabrication using the Investment Casting Process. *International Journal of Technology*, Volume 6(4), pp. 613–621

Tammas-Williams, S., Withers, P., Todd, I., Prangnell, P., 2016. Porosity Regrowth during Heat Treatment of Hot Isostatically Pressed Additively Manufactured Titanium Components. *Scripta Materialia*, Volume 122, pp. 72–76

Tsantrizos, P.G., Allaire, F., Entezarian, M., 1998. *Method of Production of Metal and Ceramic Powders by Plasma Atomization.* Google Patents

Wang, J., Kusumoto, K., Nezu, K. 2000. Plasma Arc Cutting Torch Tracking Control. *In:* Proceedings of the 6th International Workshop on Advanced Motion Control. Proceedings (Cat. No. 00TH8494), 2000: IEEE, 345–350

Zhao, S.L., Fan, J.F., Ren, S.B., Le, H.R., 2007. Gas Velocity Measurements of Close-coupled Atomizers. *In:* Proceedings of the Materials Science Forum, pp. 1819–1822